Design and simulation of a robotic arm for manufacturing operations in the railcar industry.

Available online at www.sciencedirect.com

ScienceDirect

Procedia Manufacturing 51 (2020) 67–72

Procedia MANUFACTURING

www.elsevier.com/locate/procedia

30th International Conference on Flexible Automation and Intelligent Manufacturing (FAIM2020)
15-18 June 2020, Athens, Greece.

Design and simulation of a robotic arm for manufacturing operations in the railcar industry

Ilesanmi Daniyan[a], Khumbulani Mpofu[a] Boitumelo Ramatsetse[a] Adefemi Adeodu[b]

[a]*Department of Industrial Engineering, Tshwane University of Technology, Pretoria, 0001, South Africa.*
[b]*Department of Mechanical and Mechatronics Engineering, Afe Babalola University, Ado-Ekiti, Nigeria.*

* Corresponding author. Tel.: +27727021931 *E-mail address:*afolabiilesanmi@yahoo.com

Abstract

As part of the application of the Fourth Industrial Revolution (FIR) to manufacturing activities, robotic solutions are integrated into the cyber physical systems and the production systems to enhance the automation of the manufacturing processes. This will further enhance high productivity with reduced manufacturing cycle time and overall cost. This work discusses the modelling and simulation of a robotic arm for manufacturing operations in the railcar industry. The Computer Aided Design (CAD) and the Finite Element Analysis (FEA) were carried out using the Solidworks 2017 under different loading conditions. The results of the finite element analysis showed the robotic arm is unlikely to yield or fail under different loading conditions as examined using the Von Mises failure analysis criterion. The negligible magnitude of the strain and displacement distributions imply that the robotic arm will be able to perform the gripping, handling and assembly operations with high degree of precision and accuracy during the manufacturing processes. Furthermore, using the inverse kinematics model in the MATLAB 2018 b environment, the kinematic motion and trajectory of the robotic arm along the X-Y coordinates show the movement of the robotic arm along a well-defined path, which indicates that the arm is highly flexible, characterized by smooth motion along the predetermined path during the manufacturing operations. Hence, this will promote the development of products with high quality in an efficient and fast process.

Keywords: FIR, FEA, Modelling and Simulation, Railcar, Robotic solution.

1. Introduction

With the dynamics of manufacturing activities and the advent of industrial revolutions, the manufacturing activities is becoming increasingly complex with the ever-changing customers' requirements. Hence, robotic solution plays a major role in the quest for manufacturing automation, operational efficiency, high productivity and safety [1-2]. This will assist manufacturers in the industries to gain a competitive edge. The robotic solutions often comes in various configurations depending on the degree of automation ranging from fully autonomous systems that are usually employed for high volume, dedicated and repetitive works with programs that specify the path and motion of the robot to the semi-autonomous systems which requires some level of human involvement and flexibility. Other applications of robotic solutions will assist manufacturers perform certain operations with high degree of accuracy and precision thereby reducing the margins of error and subsequent rework. Robotic solutions can be deployed for manufacturing operations such as handling, assembly or disassembly, machining and inspection operations [3-4], most especially operations that are complex, dangerous or in difficult to reach areas thereby maximizing the efficiency of operation [5-6]. The speed and

10.1016/j.promfg.2020.10.011

dexterity of robots are some of the characteristics that manufacturers often explore in manufacturing to remain competitive. In some areas where it might be difficult to recruit employees, the robot can adequately fill the skills gap offering solutions with potential cost savings. In terms of dexterity, robots can satisfactorily perform operations such as lifting, holding and placing of work pieces in a continuous or repetitive manner [7]. Furthermore, robotic solutions aids the development of a flexible and integrated manufacturing system which promotes product customization and high reproducibility with advanced sensors and camera functions for perception and environment interactions [8]. The design of robotic components and the optimization of the process parameters is essential in order to improve its performance under different operating and loading conditions [9-10]. For instance, when robots are not well configured for an operation, it might be counterproductive. Hence, its modelling and simulation at the design phase will allow the optimization of the robotic system for operational efficiency. The robotic axes are usually designed to reach any point in a plane or in space. For effective control of the robotic manipulator, three other axes such as the yaw, pitch and roll axes might be required. Many works have been reported on the modelling and simulation of robotic systems for industrial applications. For instance, Brüning *et al.* [11] reported on the simulation based planning of machining processes with industrial robot while Denkena *et al.* [12] carried out the design and optimization of a machining robot. Papakostas *et al.* [13] reported on the integration of digital manufacturing and simulation tools in the assembly design process involving cooperating robots cell case while Tsarouhia *et al.* [14] designed a robotized assembly process using dual arm robot. Makris *et al.* [15] and Michalos *et al.* [16] examined the design considerations and the challenges of cooperating robots for reconfigurable assembly operations. The findings from the works indicate that the modelling and simulation is a tool, which can assist in the determination of the optimum configurations of the robotic systems as well as the optimum path that will enhance smooth robotic motion and operation. This work examines the computer-aided design, modelling and simulation as well as the finite element analysis of the robotic arm under different loading conditions using the Solidworks software while employing the Von Mises failure analysis criterion as a basis for the determination of the behaviour of the robotic manipulator to the stress induced. The modelling and simulation of the robotic arm for manufacturing activities in the rail manufacturing industries has not been sufficiently highlighted. Hence, it is envisaged that the findings of this work will assist manufacturers most especially the railcar manufacturers in the development and application of robotic solutions to manufacturing activities in order to increase productivity and promote automation and reliability at high operational efficiency.

2. Methodology

The framework of the design and simulation of the robotic arm is shown in Fig. 1.

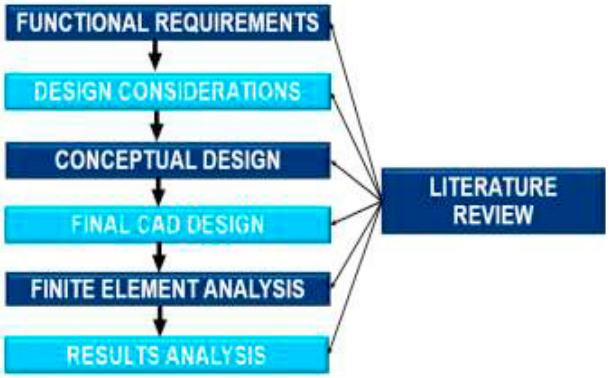

Fig. 1. The design framework for the robotic arm.

The design starts with the functional requirements of the robotic arm. The robotic arm is expected to perform gripping, handling operations with adequate pick and place capabilities as well as assembly and inspection operations of the component parts during railcar manufacturing. Next is the design considerations. The robot is also expected to possess high degree of dexterity, precision and repeatability.

The design considerations of the robotic manipulator takes into account the following;

1. The joints, which determines the kinematic motion of the robot. The reduction in joint without sacrificing the strength and efficiency of operation will improve the kinematic motion of the robot and reduce the energy requirements of the system thus making it cost effective and environmentally friendlier.
2. The payload, which determines the total weight that can be handled by the robot. The high strength to weight ratio is one of the criteria considered during the selection of materials for the robotic manipulator.
3. The degree of repeatability, which defines the distance it takes the robot to return to its programmed position. High degree of repeatability reduces the manufacturing cycle time with an increase in the productivity.
4. The degree of accuracy, which determines the ability of the robot to reach its pre-programmed position and executes the task assigned. Proper robot calibration and configuration coupled with the incorporation of advanced sensor and cameras to aid the machine vision often improves the robots accuracy.
5. Motion control.
6. Power source ranging from electrically actuated robotic manipulator to hydraulically or pneumatically actuated ones.
7. Drive mechanism.

The robotic arm is designed for use in several applications involving the gripping, handling and assembly operations. However, the payload of the arm (limited to 20 kg) selected for the mechanical loading of the arm during the modelling was informed by the average load of gripping, handling and assembly operations in the railcar manufacturing industries. Using the factor of safety, this value can be scaled up or down

to suit manufacturing operations in other industries.

The torque (T) required for the actuator to produce the turning effect is determined from Equation 1.

$$T = mgL \quad (1)$$

Where; m is the mass of the load handled by the arm (kg); g is the acceleration due to gravity (m/s^2) and L is the length of the link (m).

The magnitude of torque developed is a function of the force applied, the position or the lever arm vector, which connects the origin to the contact point where the force is applied, and the angle between the force and lever arm vectors expressed as Equation 2.

$$T = |r| \times |F| \sin\theta \quad (2)$$

Where r is the position or lever arm vector, F is the force vector which is a cross product which produces a vector which acts perpendicularly to both the position vector and the force applied and θ is the the angle between the force and lever arm (deg.).

The angular momentum (a) is related to linear momentum (p) as expressed by Equation 3.

$$a = r \times p \quad (3)$$

2.1 *The finite element analysis*

The finite element analysis of the robotic arm was carried using Solidworks 2017. The material's properties are presented in Table 1 while the meshing information is presented in Table 2.

Table 1. The material's properties of the robotic arm.

Properties	Specification and value
Material	Alloy steel
Model type	Linear elastic isotropic
Failure criterion	Von Mises stress analysis
Yield strength	6.220422E08 N/m^2
Tensile strength	7.23826 E08 N/m^2
Elastic modulus	2.10 E11 N/m^2
Poison's ratio	0.28
Mass density	7700 kg/m^3
Shear modulus	7.9 E10 N/m^2
Thermal expansion coefficient	1.30E-05/K

Table 2. Meshing information.

Mesh type	Solid Mesh
Mesher Used	Standard mesh
Jacobian points	4 Points
Element Size	23.6042 mm
Tolerance	1.18021 mm
Total Nodes	18272
Total Elements	11076
Maximum Aspect Ratio	24.445
% of elements with Aspect Ratio < 3	91.9
% of elements with Aspect Ratio > 10	0.469
% of distorted elements (Jacobian)	0

The model of the meshed sample is presented in Fig. 2.

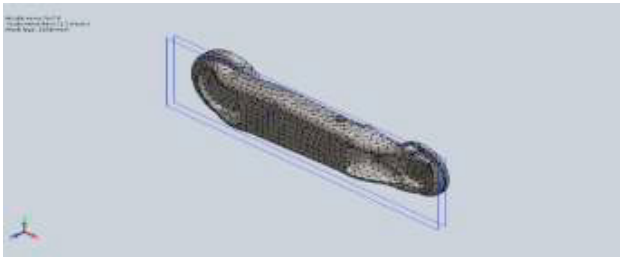

Fig. 2. The meshed sample.

The reaction forces in the X, Y, and Z directions as well as the corresponding resultant force is presented in Table 3.

Table 3: The reaction forces,

Reaction forces	Value (N)
Sum X	16.381
Sum Y	10.2931
Sum Z	-0.00279425
Resultant	19.3463

The robotic arm is subjected to different loading conditions (Fig. 3 and 4) and its behaviours under these conditions were examined.

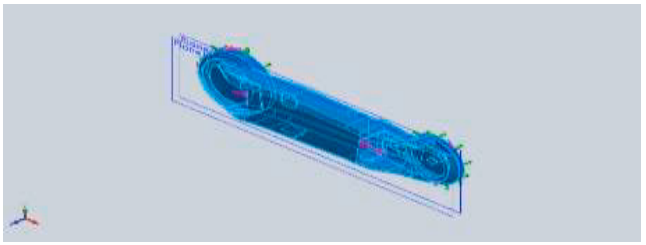

Fig. 3. The model under a maximum load of 30 kg.

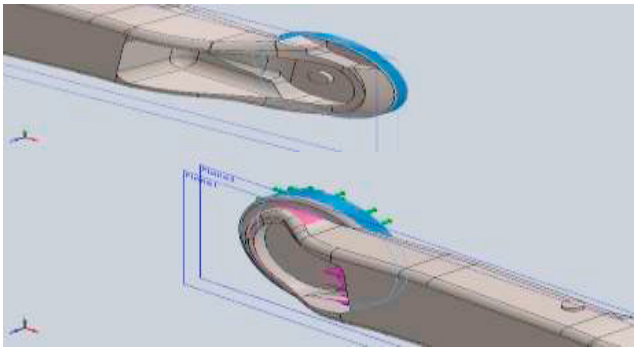

Fig. 4. The model under a varying torque of 1 Nm and 85 Nm.

2.2 *Simulation of the dual arm robot*

The finite element analysis and the simulation of the designed robotic manipulator was carried out using the Solidworks (2017) with the Von Mises stress analysis selected as the failure criterion [17-18]. This is to determine the performance of the robotic manipulator in real time vis a vis the functional and the service requirements. In addition, the

simulation also provides insight to the strength and reflexes of the robotic manipulator as well as the extent of deformation under different loading conditions. This will enhance the proper configuration of the links, angles of the joint and arrangement of location of the tip of the arm for increased flexibility.

2.3 *System's dynamics modelling*

The modelling of the dynamic behaviour of a robotic arm takes into consideration the elasticity and damping of the joints. The joints of the robot are modelled as a flexible object while the links are modelled as a rigid object to enhance satisfactory strength and rigidity. The dynamic equations of the system's dynamics led to the formulation of an algorithm for the modelling and simulation of the robotic arm which takes into account the nonlinearities of the joint drives. The motion of the robotic arm was investigated using the inverse kinematics in the MATLAB 2018 b environment. The effect of the frictional forces were considered and added to the total force on the robotic arm. The rod of the robotic arm was considered to have two circular elements having lengths l_1 and l_2, hence the total length of the elements is expressed as Equation 4.

$$L = l_1 + l_2 \quad (4)$$

The first circular element connects from the base to the contact point where the contact force f_c acts while the second elements links the tip of the finger of the robotic arm, hence, the movements can be described along the XY Cartesian coordinate.

The total angle subtended by the robotic arm (θ) is a function of the individual angle subtended by the elements θ_1 and θ_2 for the first and second elements respectively as well as the lengths of the circular elements. This is expressed by Equations 5 and 6 for the first and second elements respectively.

$$\theta = \frac{L\theta_1}{l_1} \quad (5)$$

$$\theta = \frac{(L-l_1)\theta_2+\theta_1}{l_2} \quad (6)$$

The frictional force (f_k) of the tip is expressed as Equations 7 and 8 for the two elements respectively.

$$f_k = -k\dot{\theta}_1 \quad (7)$$

$$f_k = -k\dot{\theta}_2 \quad (8)$$

The total force on the fingertip is the summation of the contact force (f_c), tip force (f_t), and frictional force (f_k) expressed as Equation 9 while the work done on the tip is the summation of the product of the forces and the perpendicular distances moved by the arm and the moment of the tip expressed as Equation 10.

$$F = f_c + f_t + f_k \quad (9)$$

$$W = f_c.\dot{r}_c + f_t\dot{r}_t - f_k(\dot{\theta}_1 + \dot{\theta}_2) + m_t(\dot{\theta}_1 + \dot{\theta}_2) \quad (10)$$

Where r_c and r_t are the radii (mm) at the contact point and tip respectively.

Equation 11 expresses the bending moment (m_b) of the flexible rod of the robotic arm with linear elasticity.

$$m_b = \frac{EI\theta}{L} \quad (11)$$

Where E is the modulus of elasticity (N/mm^2) and I is the second moment of inertia (mm^4).

Hence, the potential energy of the element is expressed as Equation 12.

$$P.E = \int_0^{\theta}\left(\frac{EI}{L}\right)\theta d\theta$$

$$P.E = \left(\frac{EI}{2L}\right)\theta^2 \quad (12)$$

The kinetic energy of the tip is expressed as Equation 13.

$$K.E = \frac{1}{2}m_c\dot{r}_c^2 + \frac{1}{2}m_t\dot{r}_t^2 \quad (13)$$

Where m_c and m_t are the masses of the contact point and tip expressed in kg respectively.

3. Results and Discussion

Fig. 5 shows the stress distribution or the robotic manipulator. Using the Von Mises stress analysis as the failure criterion, the distribution ranges from minimum value of 2.892 N/m^2 at node 7535 to maximum value of $9.975 \times 10^4 N/m^2$ at node 16566. Comparing the value of the yield strength of the material $(6.220422 \times 10^8 N/m^2)$ to the maximum stress induced under loading $(9.975 \times 10^4 N/m^2)$, it could be seen that the robotic manipulator is unlikely to yield or deform due to stress induced during the manufacturing operation. The robotic arm is also designed to incorporate the force-torque sensor to keep the applied force and the torque at the magnitude desired for the required operation. This is because when the magnitude of the force and the torque falls below the threshold, the robotic manipulator will not be able to perform the manufacturing operations as expected and when the values of the force and the torque exceeds the threshold, the work piece and the accessory tool are likely to suffer deformation, hence, the need for control. Fig. 6 shows the displacement distribution or the robotic manipulator. The distribution ranges from minimum value of 0 at node 5 to maximum value of $5.704 \times 10^{-5}\ mm$ at node 13144. The result showed that the robotic manipulator is unlikely to be displaced under different loading conditions judging from the negligible value of the maximum displacement. This insignificant displacement distribution implies that the robotic manipulator will be able to perform manufacturing operations with high degree of precision and accuracy, thus, resulting in high geometrical accuracy and improved surface quality of the assembled products.

Fig. 7 shows the strain distribution or the robotic manipulator. The distribution ranges from minimum value of 1.543×10^{-11} at element 2645 to maximum value of 2.833×10^{-7} at element 3358. The values of the strain represent the change in the orientation and dimension of the robotic manipulator due to stress. The higher the value of strain, the lower the precision and the accuracy of the robotic manipulator and vice versa. From the results obtained, the maximum value (2.833×10^{-7}) is negligible and as such, it implies that the robotic manipulator is unlikely to be undergo any permanent deformation under different loading conditions. Fig. 8 shows the kinematic motion and trajectory of the robotic arm along the X-Y coordinates. The plot shows that the movement of the robotic arm along a well-defined path, which indicates that the arm is highly flexible, characterized by smooth motion along the predetermined path during the manufacturing operations.

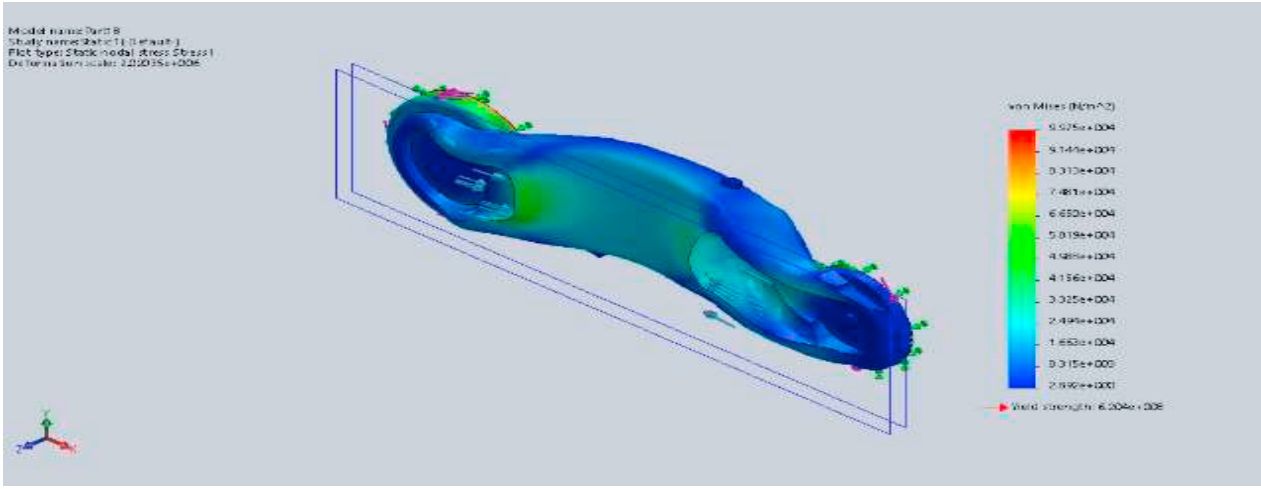

Fig. 5. The stress distribution.

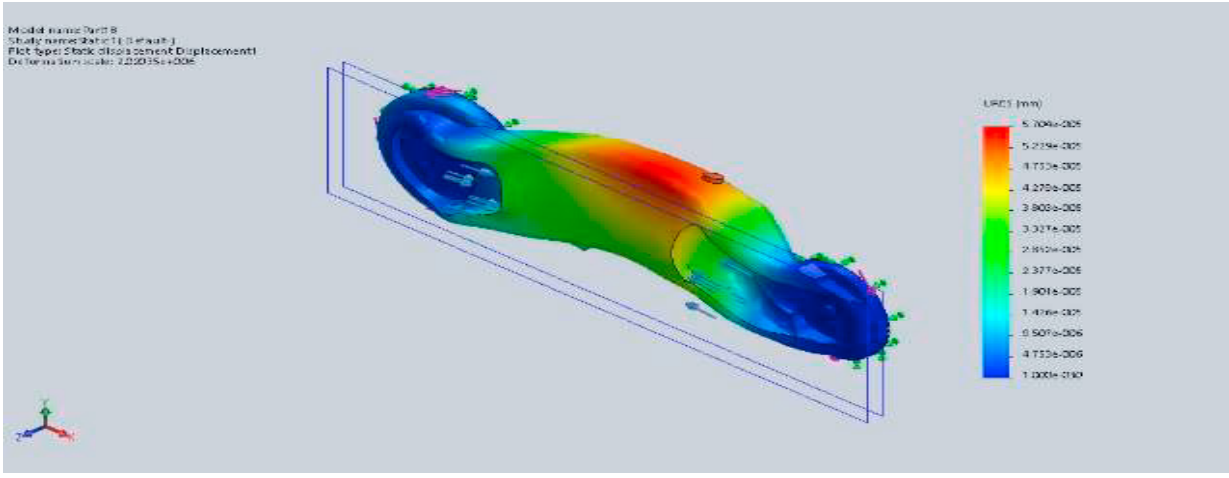

Fig. 6. The displacement distribution.

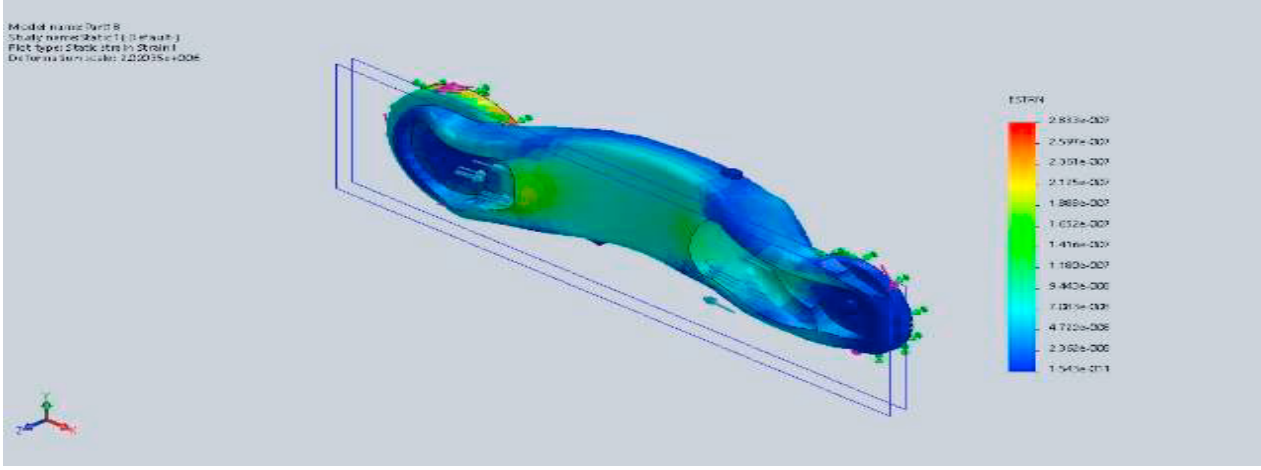

Fig. 7. The strain distribution.

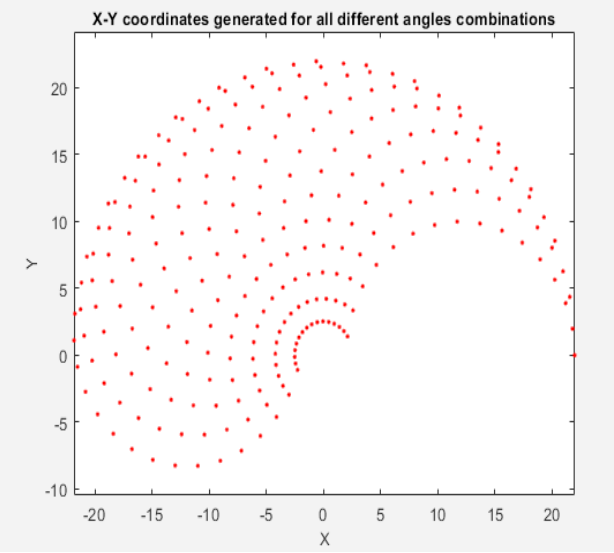

Fig. 8. The kinematic motion of the robot along the X-Y coordinates.

4. Conclusion

The design of a robotic arm for performing manufacturing operations in a railcar manufacturing industry was carried out. The design and Finite Element Analysis simulations was carried using Solidworks. The results obtained indicate that the stress induced within the robotic manipulator during loading is unlikely to cause the material to yield to stress, thereby, producing negligible strain and subsequently negligible displacement. The design will ensure satisfactory strength and flexibility during operation. The kinematic motion and trajectory of the robotic arm along the X-Y coordinates also show the movement of the robotic arm along a well-defined path, which indicates that the arm is highly flexible, characterized by smooth motion along the predetermined path during the manufacturing operations. This will increase productivity and decrease the rate of interruptions thus, promoting the automation and reliability of manufacturing activities at high operational efficiency. Hence, it is envisaged that the findings of this work will assist manufacturers most especially the railcar manufacturers in the development and application of robotic solutions to manufacturing activities in order to increase productivity and promote automation and reliability at high operational efficiency.

Future works can consider the design and simulation of the collaborations involving the robotic manipulator with the human hand.

References

[1] Chen-Gang, Li-Tong, Chu-Ming, Xuan, J.-Q. and Xu, S.-H. Review on kinematics calibration technology of serial robots, *Int. J. Precis. Eng. Manuf.,* 2014, 15(8):1759–1774.

[2] Fleischer, J., Schulze, V., Burtscher, J. and Dosch, S. Robot-based guiding of extrusion profiles-increase of guiding accuracy by considering the temperature-dependent effects. *Procedia CIRP*, 2014 18:21–26.

[3] Zaeh, M. F. and Roesch, O. Improvement of the machining accuracy of milling robots," *Prod. Eng. Res. Devel.,* 2014, 8(6):737-744.

[4] Slamani, M., Gauthier, S. and Chatelain, J-F. A study of the combined effects of machining parameters on cutting force components during high speed robotic trimming of CFRPs. *Measurement* 2015:59:268–283.

[5] Pupaza, C., Constantin, G. and Negrila, T. Computer aided engineering of industrial robots. *Proc. Manuf. Syst.* 2014, 9(2):87-92.

[6] Wang, L., Mohammed, A. and Onori, M. Remote robotic assembly guided by 3D models linking to a real robot. *CIRP Annals -Manufacturing Technology,* 2014, 63:1–4.

[7] Alexopoulos, K., Mavrikios, D. and Chryssolouris, G. ErgoToolkit: an ergonomic analysis tool in a virtual manufacturing environment. *International Journal of Computer Integrated Manufacturing*, 2013 26(5):440–452.

[8] Kah, P., Shrestha, M., Hiltunen, E. and Martikainen, J. Robotic arc welding sensors and programming in industrial applications. *International Journal of Mechanical and Materials Engineering,* 2015, 10(13):1-16.

[9] Ong, S. K., Chong, J. W. S. and Nee, A. Y. C. A novel augmented reality based robot programming and path planning methodology. *Robotics and Computer Integrated Manufacturing,* 2010, 26(3):240-249.

[10] Bugday, M. and Karali, M. Design and optimization of industrial robot arm to minimize redundant weight. *Engineering Science and Technology, an International Journal,* 2019, 22:346-352.

[11] Brüning, J., Denkena, B., Dittrich, M. A., and Park, H.-S. Simulation based planning of machining processes with industrial robots. *Procedia Manufacturing,* 2016, 6:17-24.

[12] Denkena, B., Bergmann, B. and Lepper, T. Design and optimization of a machining robot. *Procedia Manufacturing,* 2017, 14:89-96.

[13] Papakostas, N., Alexopoulos, K. and Kopanakis, A. Integrating digital manufacturing and simulation tools in the assembly design process: A cooperating robots cell case. *CIRP Journal of Manufacturing Science and Technology,* 2011, 4(1):96–100.

[14] Tsarouchia, P., Makrisa, S., Michalosa, G., Stefosa, M., Fourtakasa, K., Kaltsoukalasa, K., Kontrovrakisa, D. and Chryssolouris. Robotized assembly process using Dual arm robot *Procedia CIRP,* 2014, 23: 47-52.

[15] Makris, S., Michalos, G., Eytan, A. and Chryssolouris, G. (2012) Cooperating robots for reconfigurable assembly operations: review and challenges. *Procedia CIRP* 3:346-351.

[16] Michalos, G., Makris, S., Tsarouchi, P., Guasch, T., Kontovrakis, D. and Chryssolouris, G. Design considerations for safe human–robot collaborative work-places. *Procedia CIRP,* 2015, 37:248–253.

[17] Daniyan, I. A., Mpofu, K. Fameso, F. O. and Adeodu, A. O. Numerical Simulation and Experimental Validation of the Welding Operation of the Railcar Bogie Frame to prevent Distortion. *The International Journal of Advanced Manufacturing Technology*. 2020, 106:5213–5224.

[18] Daniyan, I. A., Fameso, F. Ale, F., Bello, K. and Tlhabadira, I. Modelling, simulation and experimental validation of the milling operation of titanium alloy (Ti6Al4V). *The International Journal of Advanced Manufacturing Technology*, 2020, 109(7):1853-1866.